STRUCTURAL INTEGRITY ANALYSIS FOR EXPOSURE TO ELEVATED TEMPERATURES IN THE POINT LEPREAU IRRADIATED FUEL BAY

H. Mohammed[1], W. Mekky[1], M. Moland[2], D. Mullin[2]
[1] AMEC Foster Wheeler Nuclear Safety Solutions, Toronto, Ontario, Canada
[2] New Brunswick Power, Point Lepreau, New Brunswick, Canada

Hesham.Mohammed@amecfw.com, Waleed.Mekky@amecfw.com,
MMoland@nbpower.com, DMullin@nbpower.com

Abstract

In response to the March 11, 2011, Fukushima Daiichi accident, Point Lepreau Generating Station performed a structural integrity analysis of its irradiated fuel bay under elevated temperatures up to and including boiling. As a typical CANDU-6 in-ground fuel bay design, the objective of the analysis was to estimate by a detailed three-dimensional nonlinear finite element analysis the sustained concrete cracking and corresponding stress state due to a beyond design basis temperature increase. This was done to obtain a more reliable simulation of the reinforced concrete structural behaviour as well as information on the structural degradation under the imposed structural and thermal loading conditions if they occur during the temperature rise of interest. A second objective was to estimate the expected leakage rate from the fuel bay due to any through wall cracking identified in the analysis. In this paper, the finite element analysis methodology and its results are discussed.

Keywords: Finite element analysis, Irradiated fuel bay, Spent fuel bay, structural integrity, IFB, SFB, LS-DYNA, reinforced concrete, thermal loading.

1. Introduction

In response to the March 11, 2011, event at Fukushima Daiichi, New Brunswick Power investigated the effects of a prolonged complete loss of Class VI electrical power and subsequent loss of cooling on the structural integrity of the Irradiated Fuel Bay (IFB) at the Point Lepreau Generating Station (PLGS). The IFB at PLGS is a large, in-ground monolithically constructed reinforced concrete water retaining structure supported directly on bedrock. Water in the IFB is cooled using a closed loop cooling circuit that includes pumps, heat exchangers with service water as a heat sink, ion exchangers, and resin traps. A loss of Class VI electrical power will disable the pumps circulating the cooling water in the IFB, possibly resulting in the cooling water reaching the boiling temperature of 100°C (212°F) if no mitigating action is taken.

2. Scope of the Irradiated Fuel Bay Assessment

The scope of the work included (a) prepare a simplified numerical model for the thermal analysis to determine temperature boundary conditions for use in the detailed stress analysis; (b) prepare a finite element model to analyze the structural integrity of the concrete structure at temperatures in excess of the design temperature limit, rising to 100°C (212°F); and (c) develop an assessment of the maximum credible leak rate following any predicted structural damage.

A plan view of the irradiated fuel bay is shown on Figure 1. The approximate limits of the structure are between lines (A) to (E3) and (5) to (7c). Assessment of the integrity of the concrete liner is not considered in this work and neither are the consequences of loss of shielding and requirements for additional mitigation.

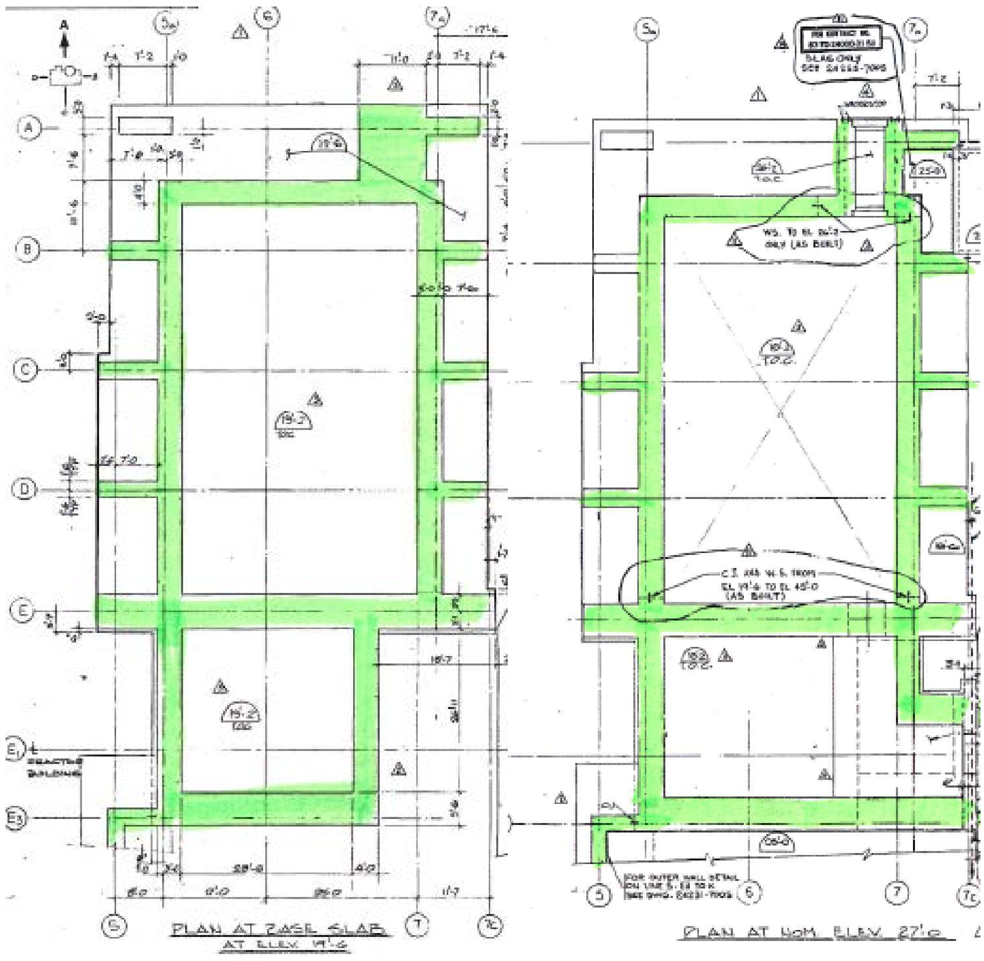

Figure 1: Plan view of RC walls at different elevations

2.1 Material Properties & Analysis Assumptions

The effects of elevated temperature on the properties and behavior of aged concrete are fairly complex due to the fact that concrete is comprised of a number of constituents that exhibit different mechanical properties. Moreover, moisture content and porosity of the concrete matrix can have an effect on the concrete mechanical performance at elevated temperature. NUREG/CR-6900 [1] provides a comprehensive review of the effects of elevated temperature on concrete with consideration to a variety of parameters. However, the European Code EN 1992-1-2:2004 [2] which is intended for the design of concrete structures for fire conditions, provides conservative and reliable recommendations pertaining to the suggested properties of reinforced concrete at elevated temperature.

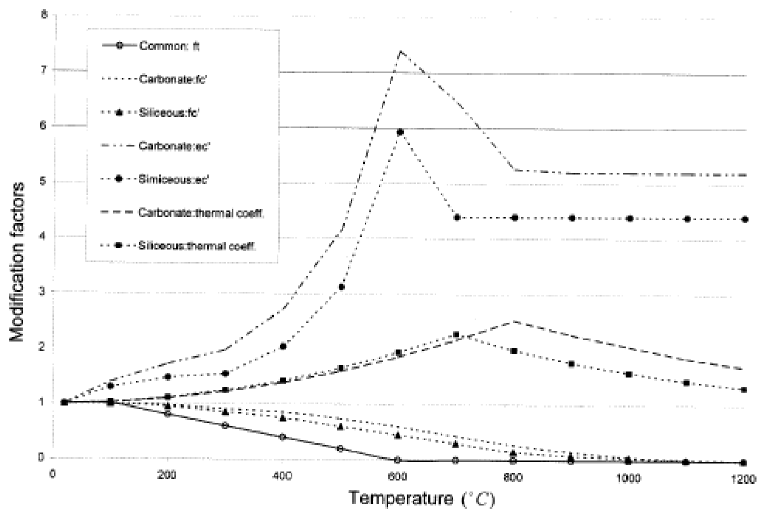

Figure 2: Modification Factors for Concrete Properties with Temperature Rise [3].

Figure 2 [3] graphically summarizes the provisions of the European code EN 1992-1-2:2004 for concrete mechanical properties with different aggregate types up to a temperature of 1200°C (2192°F). It is noted that regardless of the aggregate type, the concrete's compressive and tensile strengths can be considered constant up to 100°C (212°F), which is the temperature limit of interest in the current scope of work. Therefore, the following assumptions, conditions and material properties are considered in the finite element analysis:

1. Table 1 lists elastic material properties considered in the analysis. These properties are primarily obtained from design manual and calculations [4] and [5]. Other properties are derived based on ACI formulae [6].

Table 1: Concrete and Steel Reinforcement Properties at 20-100°C (70-212°F),

Material Property	**Value**
Coefficient of Linear Thermal Expansion (a_c)	9.2×10^{-6}/°C
Concrete Compressive Strength (f'_c)	27.6 MPa (4000 psi)
Modulus of Elasticity of Concrete (E_c)	28.82 GPa (3.6×10^{6} psi)
Yield Strength of Steel Reinforcement (f_y)	413.6 MPa (60000 psi)
Modulus of Elasticity of Reinf. Steel (E_s)	200 GPa (29×10^{6} psi)

2. The epoxy liner cannot typically be maintained beyond temperature of 65°C. It is therefore assumed that since the maximum temperature considered for the inelastic analysis is 100°C (212°F), the integrity of the epoxy liner will not be maintained and hence the epoxy liner is not modeled or considered in the finite element analysis.

3. Alkali Aggregate Reaction can have a significant impact on Concrete strength [7], [8]. There are currently no known records indicating degradation due to such a reaction in the irradiated fuel bay. Therefore, it is not considered in the inelastic finite element analysis.

4. Other than the effects of mechanical loads due to the hydrostatic pressure of the water, the weight of the floor steel liner and the weight of the spent fuel bundles and the storage trays, no other residual stresses, or pre-stress or preloading conditions are considered to exist in the reinforced concrete structure for the purpose of the analysis.

5. A steady state heat transfer is assumed to occur for the coupled thermal structural analysis due to the slow temperature rise of the IFB large water volume. The preliminary transient thermal analysis is performed using LS-DYNA to obtain the outer wall temperature based on an initial outer temperature of 6.67°C (44°F) as per references [4] and [5]., The stress free temperature of the structure is conservatively assumed to be 6.67°C (44°F) for the coupled thermal structural nonlinear finite element analysis.

6. The lifetime radiation dose is assumed to be $3x10^{10}$ rads over 50 years based on some previous estimates for the irradiated fuel bay. The affected zone at this dosage order of magnitude is assumed to be the inner concrete cover of the irradiated fuel bay, which is the closest concrete to the submerged spent fuel bundles.

7. For the tensile strength of the concrete, according the PCI Journal special report on cracks and crack control in concrete structures [9], the mean direct tensile strength f'_{tm} as related to the 28 day cylinder compressive strength f'_c is defined to be $f'_{tm}=2.1(f'_c)^{2/3}$ in units of (psi). For a compressive strength of 4000 psi, this gives a mean tensile strength of 529.3 psi which represents 13.2% of the compressive strength. For the inner concrete cover the tensile strength value corresponding to a compressive strength of 3200 psi is considered to be 456 psi based on the same formula. This is consistent with the general expectation that the tensile strength of concrete is between 10% and 20% of the compressive strength.

8. The reinforced concrete base slab is conservatively assumed to be bonded to the underlying layer of 2000 (psi) plain concrete. The plain concrete layer bottom surface nodes are considered perfectly interlocked with the underlying bedrock layer and therefore the nodes on that surface are conservatively considered fixed [10].

9. For the exterior lateral boundary condition of the irradiated fuel bay a coefficient of horizontal soil subgrade of 460 (pci) is used which is a typical value for gravel and sandy gravel backfill. This lateral confining effect is felt by the structure when the structure starts to laterally expand under the longitudinal thermal effects.

2.2 Finite Element Modelling of Irradiated Fuel Bay Structure

The strength of concrete under multi-axial stresses is a function of the state of stress and cannot be predicted by limitations of simple tensile, compressive and shearing stresses independent of each other. Therefore, the strength of concrete elements can only be properly determined by considering the interaction of the various components of the state of stress. When the state of stress reaches critical value, the concrete can start failing by fracturing. The fracture of concrete can occur in two different forms. One is by cracking, under tensile type of stress states, and the other by crushing under compressive types of stress states. The tensile weakness of concrete is a major factor contributing to the nonlinear behavior of reinforced concrete structural elements.

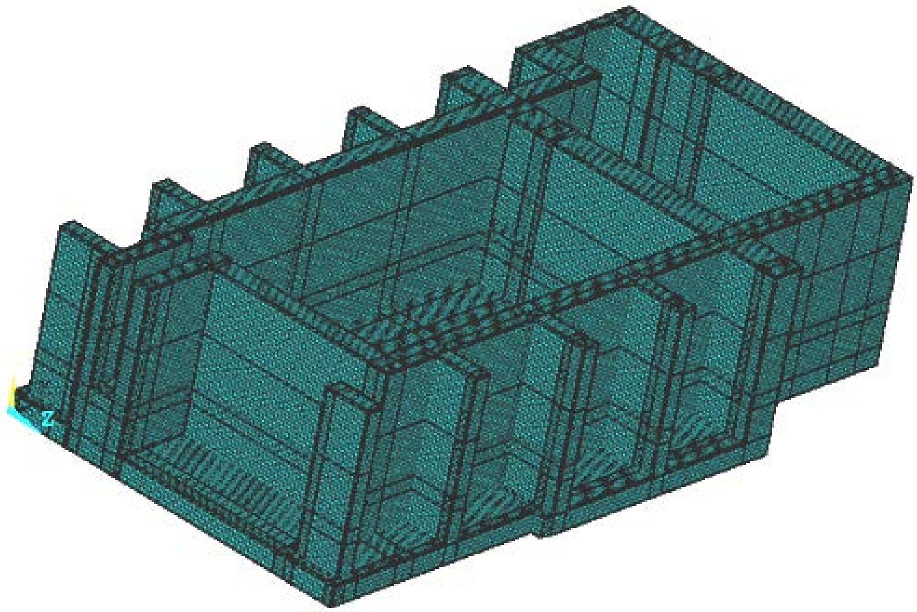

Figure 3: Isometric of Generated Point Lepreau Irradiated Fuel Bay Solid Element Discretization

Figure 3 shows an isometric view of the generated solid element model of the irradiated fuel bay based on details [10]. The generated solid element model discretization is solved in the LS-DYNA finite element software program. A specialized concrete material formulation is used to perform the coupled thermal-structural analysis. In the LS-DYNA program, the Winfrith concrete model had been developed over the last decade, and validated against a wide range of impact and blast experimental tests. The Winfrith concrete model is a smeared crack (sometimes known as pseudo crack) implemented in 8-noded single integration point continuum element. The hydrostatic stress state in the concrete is determined from a typical non-dimensional volume compaction curve. The conical yield surface along with its radii in this model expands with increasing hydrostatic stress, for the given compressive and tensile strengths. As a planar tensile crack propagates through a medium, the split medium opens and a gap is formed by the progressing crack. The size of this gap can be characterized by the crack width which is also termed as the Crack Opening Displacement (COD) or the associated crack opening angle (COA) which is related to the COD via the crack length as shown in Figure 4.

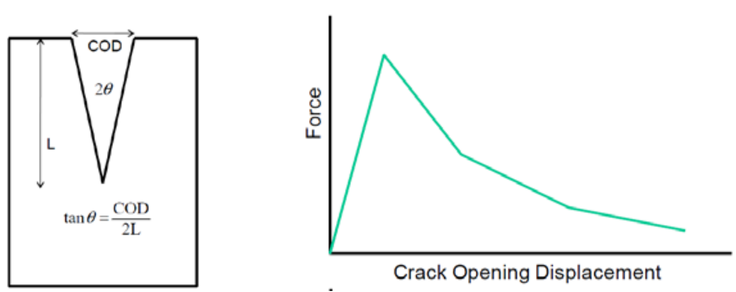

(a) (b)

Figure 4: (a) Illustration of crack opening displacement and angle. (b) Measured forces versus displacement

The crack width formulation used in the Winfrith (*MAT085) concrete model is based on the work of Wittmann, et al. (1988) [11]. Wittmann measured the specific fracture energy, crack opening displacement and maximum load for a large number of concrete samples with varying aggregate size, compressive strengths, loading rates, water-to-cement ratios, and test specimen sizes. The results of Wittmann's measurements are force versus displacement variations. The area under this curve is the work done on the specimen. Using a technique based on the *fictitious crack model* the force-displacement data is transformed into stress versus displacement.

2.3 Thermal Analysis for Determination of the Irradiated Fuel Bay Outer Wall Temperature

The scope of the thermal transient analysis for the through wall model having combination of concrete, foam layer and soil is to represent the actual temperature distribution developed across the bay wall thickness during bay water heat up in the event of Class IV power loss. A similar temperature distribution is to be estimated across the bay bottom slab for the combination of concrete and underlying rock only. Table 2 lists different material thermal properties inputs in this analysis.

Table 2: Material thermal properties

Material Property	Soil	Foam	Concrete
Heat Capacity BTU/(°F.lb)	0.21496	0.35826	0.179134
Thermal Conductivity BTU/(sec.in.°F)	$3.982X10^{-6}$	$7.72x10^{-7}$	$2.5x10^{-5}$

Two wall slice models were developed in the LS-DYNA representing a section through the retaining wall and another section through the bottom slab. Figure 5 illustrate isometric views of these models. The concrete wall and slab thickness is 4 feet in both models and the foam insulation thickness is 3 inches. Soil/rock material was taken to be 5 feet thick in both models. The inside temperature of the bay structure is ramped up from 20°C (70°F) to the water boiling temperature of 100°C (212°F). The outer soil temperature is ramped up from 6.67°C (44°F) and increases based on the transient analysis.

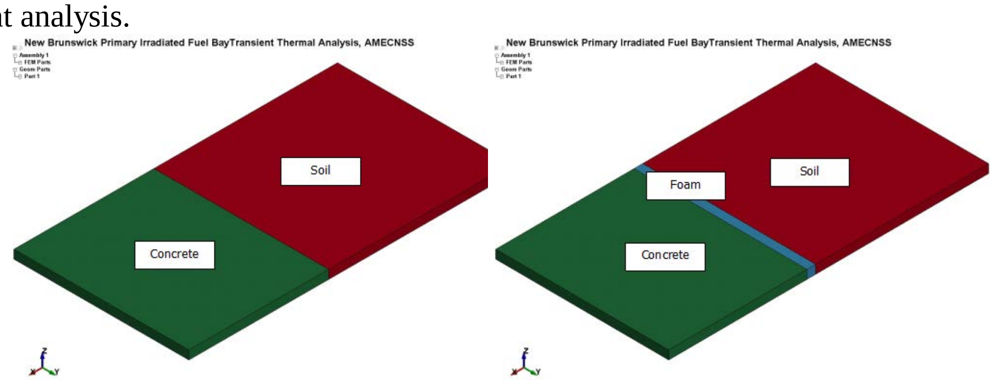

(a) (b)

Figure 5: (a) Thermal transient analysis model for the irradiated fuel bay bottom slab
(b) Cross sectional view of the irradiated fuel bay walls for Thermal transient analysis

Transient thermal analysis was performed for both models while ramping up the inside wall temperature to 100°C (212°F). Figure 6 shows the temperature distribution for the concrete wall profile after reaching the steady state conditions and shows the distribution for the bottom slab. Having the foam layer as an insulation from the outside soil resulted in heat trapping and therefore the outside wall temperature is higher than the corresponding bottom slab temperature. The underlying bedrock is assumed to act as a heat sink. Different rates are considered based on the reported cases in [12]. Two outer wall temperature values were subsequently selected as upper and lower cases. In the higher temperature case, the outside wall temperature reached 86.6°C (188°F). In the lower wall temperature case, the temperature was 72.2°C (162°F). For the bottom slab model the final outside surface concrete temperature was taken as 54.9°C (139°F).

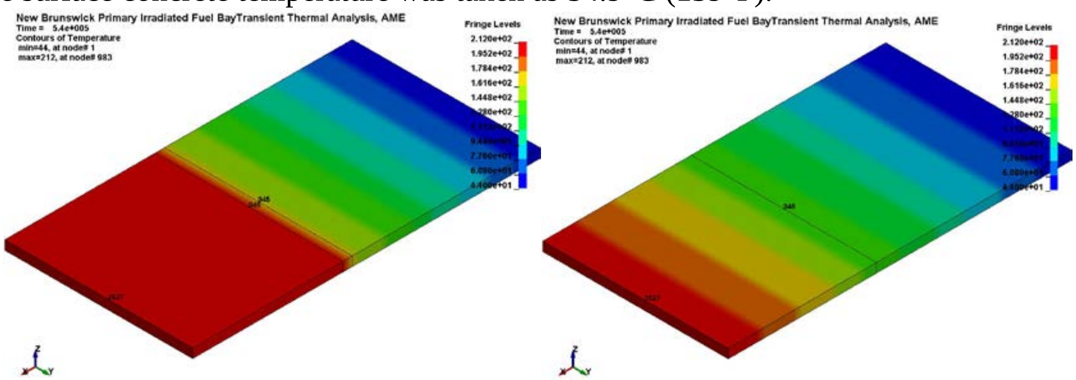

(a) (b)

Figure 6: (a) Temperature Distribution for Bay Wall Model (b) Temperature Distribution for the bottom slab model

2.4 Inelastic Coupled Field Analysis Invoked Solvers in the FE Analysis:

In the LSDYNA, the implicit solver was invoked for this analysis. Automatic time stepping was invoked in the analysis to facilitate solution convergence for the highly nonlinear problem. Double precision setting was assigned for the problem solution.

2.5 Discussion of Finite Element Results from LS-DYNA

In the current analysis, two thermal boundary condition cases are considered where the irradiated fuel bay water temperature is considered to rise to 100°C (212°F):

i. Case 1: The outside temperature rises to 86.6°C (188°F) whilst the inside surface temperature simultaneously increases to 100°C (212°F) linearly in a steady state heat transfer analysis performed in LS-DYNA. Therefore, the temperature differential in this case is $\Delta T=13.4°C$ across the irradiated fuel bay reinforced concrete wall.

ii. Case 2: The outside temperature increases to 72.2°C (162°F), whilst the inside surface temperature simultaneously increases to 100°C (212°F) linearly in a steady state heat transfer. Therefore the temperature differential in this case is $\Delta T=27.8°C$ across the irradiated fuel bay reinforced concrete wall.

For each of the studied cases, 1st, 2nd and 3rd principal stress distributions across the irradiated fuel bay wall and slab thickness, and the extent of crack propagation, are provided. The primary reason for selecting principal stresses in the current presentation is that concrete as a quasi-brittle material is expected to crack when one of the principal stresses at the current surface reaches the value of the tensile strength. When this occurs the crack propagates and a stress redistribution results in the finite elements of the model. For illustration purposes, only the 3rd principal stress distributions are shown for each case in Figure 7 and Figure 8.

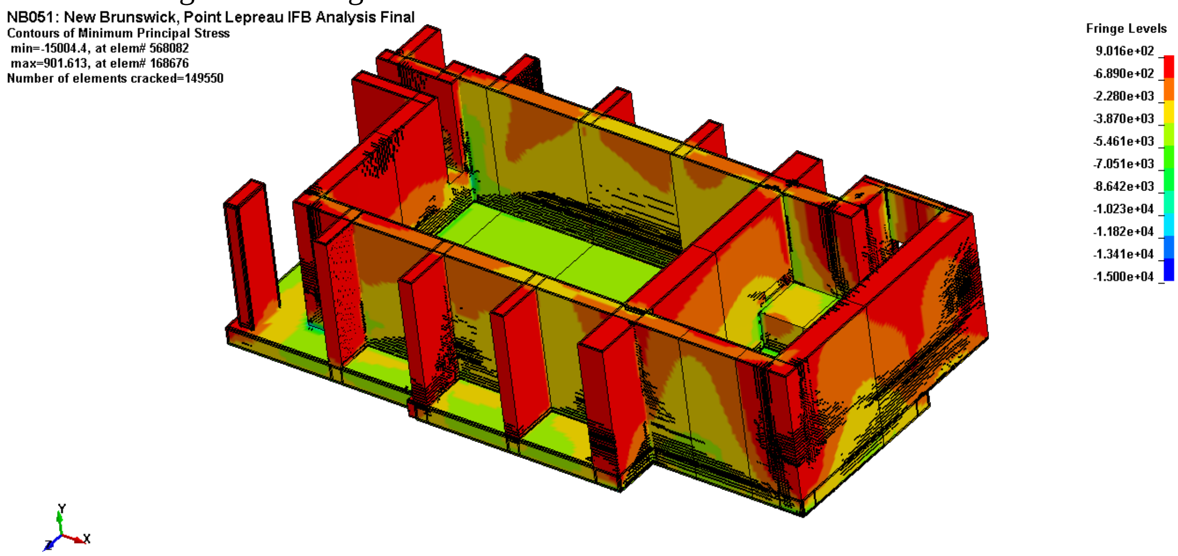

Figure 7: Case 1 - Initial 3rd Principal Stress State with Mechanical Loading and Thermal Loading Considering Outside Temperature Wises to 86.6°C (188°F) and Irradiated Fuel Bay Water Temperature Rise to 100ºC (212ºF)

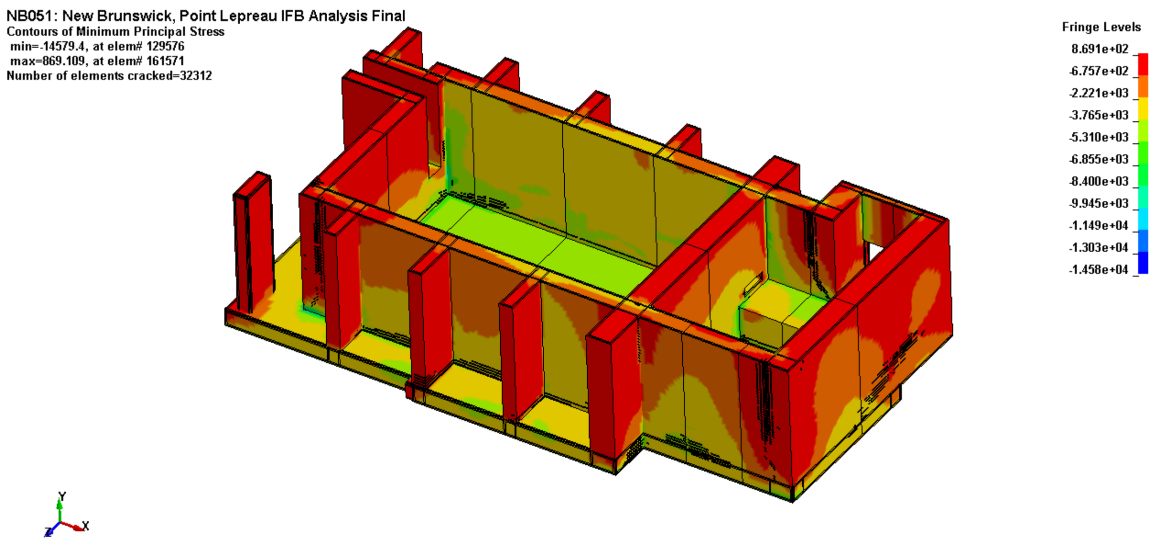

Figure 8: Case 2 - Initial 3rd Principal Stress State with Mechanical Loading and Thermal Loading Considering Outside Temperature Wises to 72.2°C (162°F) and Irradiated Fuel Bay Water Temperature Rise to 100ºC (212ºF)

The following observations are made in the analysis:

i. For Case 1, the principal stresses with imposed sustained cracking (if any) shows that the Point Lepreau irradiated fuel bay is virtually uncracked under internal mechanical and hydrostatic loading as well as external soil pressure loading conditions and prior to the introduction of thermal loading.

ii. The difference between the average temperature of the bay walls and the average temperature of the bottom slab is greater for Case I than Case II and therefore Case I is found to be more critical.

iii. It is evident that Case 1 produces higher principal stresses than Case 2 which can be explained by the higher longitudinal thermal effect component due the smaller margin between the outer and inner surfaces of the irradiated fuel bay walls. It should be noted as well in this regard, that based on the proposed formula in[13], the theoretical confined compressive strength of concrete is estimated by the formula $f'_{con} = f'_{c}+(k.s_{con})$. Where $f`_{c}$ is the uniaxial compressive strength of the irradiated fuel bay concrete at 4000 psi. The factor k ranges between 4 to 7, and is conservatively herein taken to be the lower limit 4. The confinement stress can be assumed to be the average of the two lower principal stress values. Therefore for thermal load case 1, the confinement stress is (2660+6637)/2=4648 psi. The corresponding confined strength of the concrete under triaxial compression is [4000+(4 x 4648)] = 22592 psi. This explains why although there is observed surface cracking in tension, there is no crushing of the concrete in compression for the considered thermal load cases.

iv. It is also observed that the thermally induced cracking generally begins on the cooler side of the irradiated fuel bay walls (outside) and propagates inwards, during temperature rise to 100°C (212°F). Thermal stresses induced in highly indeterminate reinforced concrete structures tend to be dissimilar to most other mechanical stresses in that they tend to be self-relieving to some degree. The magnitude of thermal stress induced is partially governed by the effective stiffness of the member as well as geometrical discontinuities. As cracks develop and propagate within the concrete, the effective stiffness of the member is reduced, thus causing a relaxation in the thermal flexural moments. The combined thermal and mechanical loads cause more cracking at intersections of structural elements and locations that are more restrained due the fact that these locations represent geometrical discontinuities which aids in stress concentration and therefore initiating the crack.

v. There is a general observation that cracking in the studied cases is largely concentrated at the base of the retaining walls of the irradiated fuel bay. However, it should be noted that in the current modeling a conservative boundary condition is applied to the base of the reinforced concrete slab by assuming it is virtually bonded to the underlying plain concrete layer which in turn is assumed fully interlocked with the bedrock.

vi. A reinforced concrete structure subjected to thermal loads will develop stresses as a result of the restrained thermal expansion. In continuous structures such as the Point Lepreau irradiated fuel bay, two components of thermal stress can generally be identified. The first are the primary thermal stresses which result in sections where thermal gradients exist. These stresses are self-equilibrating across the section of the walls and slabs of the irradiate fuel bay. They arise due to the incompatibility between the two requirements that plane sections remain plane and that the unstressed fibers expand by an amount proportional to the local temperature rise.

vii.

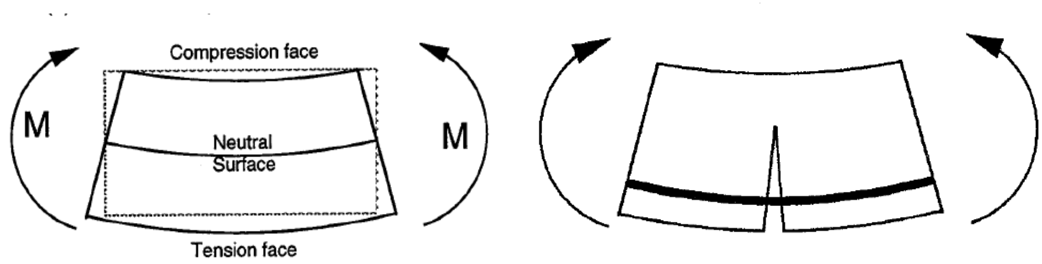

Figure 9 (a) Elastic deformed structural member under flexure (b) Deformed cracked reinforced concrete member under flexure

Figure 9 (a) shows the typical starting location of the neutral axis (neutral surface) location for an uncracked section. For a cracked section such as in Figure 9(b), the neutral axis moves to just above the crack tip. Continuity thermal stresses on the other hand, are stresses occurring in statically indeterminate structures due to the restrained members deflections and rotations which result from thermal deformations of the structure, (e.g. such as the supporting base slab of the irradiated fuel bay).

viii. The cracking pattern particularly at the base of the retaining walls implies that the differential longitudinal displacement due to thermal expansion of the upper walls is more than that of the supporting base slab. In addition the supporting base slab is generally at a lower temperature due to the absence of insulation. It is important to note that not all the cracks appearing on the exterior surface of the irradiated fuel bay penetrate through the wall to the interior surface. To clearly identify which cracks are considered more critical and contributing to leakage, the confined concrete core is examined for Case 1 thermal loading. Eurocode2-part3 [14] indicates that through wall cracks having a width of 0.2mm or less are unlikely to result in leakage provided the hydrostatic head to wall thickness ratio ($h_D/h \leq 5$). The limit is 0.05mm where ($h_D/h \geq 35$). Interpolation is permitted between the two limits. For the Point Lepreau irradiated fuel bay the interpolated crack width value is determined to be 0.193mm (0.0076”).

3. Conclusions

Both analyzed beyond design basis thermal load cases indicate that the most significant cracking affecting the confined concrete develops at the base of the retaining walls at the interface with the bottom slab. At this geometric discontinuity it is generally believed that the geometry in combination with the assumed fixed boundary conditions, give rise to higher crack initiating stresses which help the crack development to dissipate this strain energy. Not all the examined irradiated fuel bay segments indicate the development of a through wall crack that can lead to leakage. In both thermal loading cases, only 5 out of the 14 segments developed through wall cracks that could result in leakage as demonstrated by the leakage estimate. The current analysis provides a prediction for the short term exposure of the Point Lepreau irradiated fuel bay from the normal operating temperature range to a temperatures reaching 100°C (212°F) based on the analysis assumptions. The prolonged exposure to the 100°C (212°F) on the other hand may result in further alteration in the chemical structure of the concrete matrix through effects such as dehydration. Such effects in turn may alter mechanical properties of the concrete [1]. The prolonged exposure is not studied in the current scope of work.

4. References

[1] NRC Report No. NUREG/CR-6900 (ORNL/TM-2005/553), titled "The Effect of Elevated Temperature on Concrete Materials and Structures – A Literature Review," dated 2006

[2] European Code EN 1992-1-2 titled "Design of Concrete Structures – Part 1-General Rules – Structural Fire Design," dated 2004.

[3] Vecchio F.J., Zhou C.E., "Nonlinear Finite Element Analysis of Reinforced Concrete Structures Subjected to Transient Thermal Loads," Computers and Concrete, Vol.2, No. 6 , page 455-479, 2005.

[4] DM-5061-24000-01 Rev.01, titled "PLGS Design Manual, Service Building," dated June 1982.

[5] DK-5061-24250-01, titled "PLGS Design Calculations Service Building Spent Fuel Bay – Reinforced Concrete", November 1980.

[6] Nawy E., "Reinforced Concrete, A Fundamental Approach," 5th Edition to ACI 318-05 Code Edition, 2005.

[7] Pietruszczak S., "On The Mechanical Behaviour of Concrete Subjected to Alkali Aggregate Reaction," Computers and Structures, Vol. 58, No. 6., page 1093-1097, 1996.

[8] Huang M., and Pietruszczak S., "Modeling of Thermomechanical Effects of Alkali-Silica Reaction," Journal of Engineering Mechanics, page 479-485, 1999.

[9] Leonhart F. "Cracks and Crack Control in Concrete Structures," Special Report – PCI Journal, July-August 1988.

[10] DWG # 87-24154-7001-01-DD-E Rev.05, titled "Service Building Spent Fuel Bay Under drainage Plan and Sections," dated April 1975

[11] Wittmann, F.H., K. Rokugo, E. Bruhwiler, H. Mihashi, and Ph. Simonin, "Fracture Energy and Strain Softening of Concrete as determined by means of Compact Tension Specimens," Materials and Structures, Vol.21, 21-32, 1988.

[12] IR-35360-01 Rev.01, titled "Assessment of Storage Bay Events," dated July 16th 2012.

[13] Aldea C. Et. Al., "Estimation of Water Flow through Cracked Concrete under Load," ACI Materials Journal, title no. 97-M65, page 567-575, September-October 2000.

[14] Eurocode-2 Part 3 titled "Liquid Retaining and Containment Structures," dated October 2004.